Metastable excited states of a closed quantum dot probed by an aluminum single-electron transistor

J. C. Chen,[1,2] Zhenghua An,[1,2] T. Ueda,[1,2] S. Komiyama,[1] K. Hirakawa,[3] and V. Antonov[4]
[1]*Department of Basic Science, University of Tokyo, Komaba 3-8-1, Meguro-ku, Tokyo 153-8902, Japan*
[2]*Japan Science and Technology Corporation (JST), Kawaguchi-shi, Saitama 332-0012, Japan*
[3]*Institute of Industrial Science, University of Tokyo, Komaba, Meguro-ku, Tokyo 153-8505, Japan*
[4]*Physics Department, Royal Holloway University of London, Egham, Surrey TW20 0EX, United Kingdom*
(Received 17 November 2005; revised manuscript received 20 January 2006; published 24 July 2006)

Kinetics of a closed quantum dot (QD) in a GaAs/AlGaAs heterostructure crystal are studied by probing the current through an aluminum single-electron transistor fabricated on top of the QD. Distinctly different characteristics of the Coulomb blockade oscillations are found in different gate bias conditions, indicating different regimes of the isolated QD. An excited state of the QD, where the electrostatic potential is significantly lifted up, as well as another excited state, where the electrostatic potential is significantly pulled down, are suggested. Both of the states are characterized by an extremely long life time roughly about 20 min. A model is proposed to consistently explain these states.

DOI: 10.1103/PhysRevB.74.045321 PACS number(s): 73.23.Hk

The physics of semiconductor quantum dots (QDs) formed electrically by metal gates have been extensively studied via the tunnel current passing through the QDs. Recently, closed QDs, the tunnel coupling of which to the electron reservoirs is completely turned off, attracted considerable attention.[1–4] The researches are motivated primarily by the interest of applying QDs as an electrical element for storing and/or processing quantum information, which naturally leads to the fundamental interest of dephasing mechanism in such isolated QDs. Simply considered, isolation of a QD is the basis for avoiding unwanted mechanisms of decoherence. Specifically, it is a prerequisite for the quantum bits (qubits) to isolate an electrical element for a certain period of operation time. For many other applications the control of closing and opening the tunneling path through a QD may be necessary. Once a QD is electrically isolated, one needs a physical probe (other than the tunneling current) to access the information stored in the QD; for instance, a quantum point contact (QPC) or a single-electron transistor (SET) placed nearby the QD will serve as an electrometer to probe the QD.[1,2,5,6] To date, the kinetics of how the isolated QDs are formed by biasing the surrounding metal gates are not very well understood. Particularly, it is suggested that the total energy of the QD is raised during the building up process of the isolated QD.[5] However, the whole process of closing and reopening the QD is not fully clarified, and values of the relevant energies have not been figured out quantitatively.

Here we study evolution of the excited state of a closed QD by monitoring the tunnel current passing through an aluminum (Al) SET fabricated on top of the QD. Owing to the large capacitive coupling to the QD, Al SET provides a sensitive probe to the QD.[7–9] It is important that Al SET continues to detect electrostatic conditions of the QD while the conducting channel through the QD is completely turned off. During the processes of closing and reopening the QPCs for the QD, Al SET exhibits distinctly different patterns of Coulomb blockade (CB) oscillations, from which we figure out several important physical parameters characterizing the QD.

Figure 1(a) is a scanning electron beam micrograph of the device, in which an $Al/AlO_x/Al$ superconducting SET is fabricated on top of a semiconductor QD. The QD is fabricated in GaAs/AlGaAs heterostructure containing two-dimensional electron gas (2DEG) 90 nm below the surface with an electron concentration of $n=2.68\times10^{11}$ cm^{-2} and an electron mobility of $\mu=1.23\times10^{6}$ cm^2/V s at 4.2 K, respectively. The QD is formed by biasing the metal gates, which consist of the main gate (M), the pincher gates (1 and 2), and the plunger gate (p). These metal gates are patterned by electron beam lithography, while Al SET is fabricated by a standard shadow evaporation technique.[10] The device is placed in a ^{3}He/^{4}He dilution refrigerator with a base temperature of 70 mK. A special care is taken to shield the device from external electromagnetic radiation. The formation of the respective QPCs, QPC $M1$ and QPC $M2$, are confirmed by the steps of quantized conductance plateaus as shown in Fig. 1(b). The charging energy of the QD in a condition with a finite tunnel conductance through the QD is derived from the standard CB oscillations to be $U_c=e^2/C_\Sigma=0.61$ meV. The effective electron temperature of the QD is estimated from the width of the conductance resonance peak in the CB oscillation to be approximately 100 mK. Figure 1(c) shows the I-V characteristics of Al SET, taken in the condition when all the metal gates and the 2DEG are grounded. The charging energy of the SET is estimated to be approximately $E_c \sim 250$ μeV from the I-V characteristics of Al SET in the normal state. Below we designate the conductance through the QD as G_d, and the current through Al SET as I_s. To confirm that the device works properly, we first fix the bias voltages, V_M, $V1$ and $V2$, to the gates M, 1 and 2, so that the QD is formed but not isolated (or the conductance through the two QPCs is small but finite), and study G_d and I_s as a function of the bias voltage V_p on the plunger gate p. The equivalent circuit is illustrated in Fig. 1(d). A low-frequency ac voltage $V_{rms}=20$ μV (17 Hz) superposed on the dc bias voltage ($V_{bias}=850$ μV) is applied to the source contact to Al SET, where the drain lead for Al SET is grounded commonly with the QD. The dc bias voltage is chosen so that Al SET is operated at the Josephson-quasiparticle (JQP) peak,[11] where

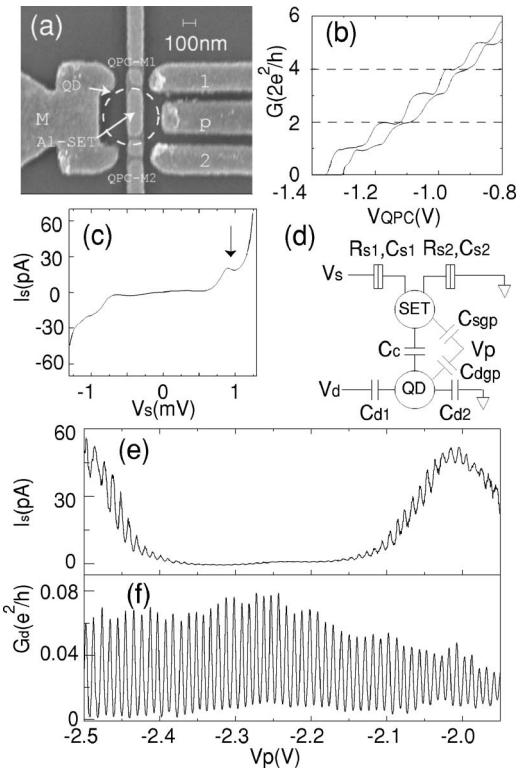

FIG. 1. (a) A scanning electron micrograph of the device. The lithographic size of the QD is 560 nm×570 nm. (b) Characteristics of the two QPCs. The lower and the upper traces are for QPC $M1$ and QPC $M2$, respectively. (c) I-V characteristics of Al SET. The sharp rise of I_s at 1.13 mV suggests $\Delta=282$ μeV. A small peak marked by the arrow (892 μV) is due to the JQP cycle. (d) A circuit diagram used to model coupled SET dot system. The relevant parameters deduced from the experiments are $C_{sgp}=0.27$ aF, $C_{dgp}=13.3$ aF, $C_{s1}\sim C_{s2}=320$ aF. C_c is estimated to be 58.8 aF. The normal resistance of Al SET is $R_{s1}+R_{s2}\sim 624$ KΩ. (e) The current through Al SET at $V_{bias}=850$ μV. (f) The zero-bias CB oscillations in the QD with the same gate bias conditions as for (e).

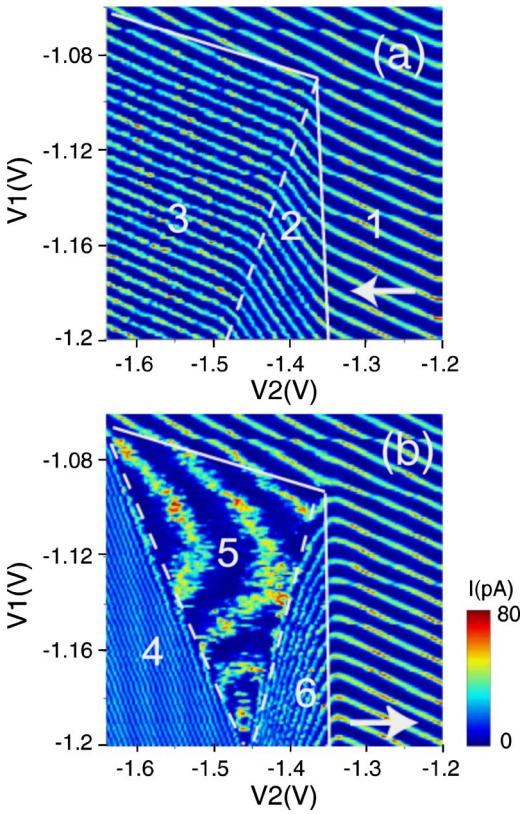

FIG. 2. (Color online) Plots of the CB oscillation patterns of Al SET, displayed in the $V1$-$V2$ plane. The arrows mark the direction of scanning $V2$ for (a) and (b), where $V1$ varies stepwise after each scan, which takes 2 min. The solid and the dotted white lines are drawn to separate different regions.

the highest sensitivity is expected.[12]. Figures 1(e) and 1(f) display I_s and G_d against V_p, respectively. In the curve of I_s, a short-period (~10.8 mV) oscillation, small in amplitude, is superposed on a longer-period (~500 mV) larger-amplitude oscillation. The curve of G_d is featured by a single, short-period CB oscillation, which is found to coincide with the short-period small-amplitude oscillation in I_s.[8] Though not shown here, the short-period oscillation in I_s is found to disappear if one of the QPCs is more open so that the CB oscillations of the QD vanishes. These features make it certain that the short-period oscillation in I_s originates from the change of the number of electrons, N_{QD}, in the QD by one, while the long-period oscillation in I_s comes from the change of the number of electrons, N_{SET}, in the Al island of Al SET by one. From the measurements here the charge sensitivity of the SET is estimated to be approximately $\delta q=3.68\times 10^{-4}e/\sqrt{Hz}$.

We now study I_s in the condition where the QD is closed. Figures 2(a) and 2(b) display two-dimensional plots of the CB patterns of Al SET obtained by scanning the gate bias voltages $V1$ and $V2$, where $V_p=-1.439$ V and $V_M=-1.304$ V are fixed. The data are taken by scanning $V2$ at a fixed value of $V1$, which increases from −1.2 V to −1.06 V at a step of 0.25 mV. The direction of scanning $V2$ is opposite between Figs. 2(a) and 2(b) as indicated by the white arrows. Conductance resonance peaks in the CB oscillation, visible as the traces of bright regions, occur each time when the number of electrons in the Al island of Al SET changes by one. [The conductance is weakly modulated by the change of the number of electrons in the QD, but is not clearly discerned in the presentation of Figs. 2(a) and 2(b).] The pattern of CB peaks is largely different according to the scan direction. In addition, we note distinctly different regions, 1 through 6, which we separate with white solid lines and white dashed lines. Though not shown here, the measurements of G_d shows that the QD is electrically isolated ($G_d=0$) in the lower left regions to the white lines (regions 2 through 6) while it is weakly coupled to the reservoirs in region 1. The scan-direction dependent patterns show up only in regions 2 through 6, where the QD is isolated. The features of I_s are described in more details below by taking the traces obtained at $V1=-1.2$ V as an example. Figures 3(a) and 3(b) display the typical two traces. In Fig. 2(a) and 3(a), I_s in region 1 oscillates smoothly without exhibiting any irregular feature. As $V2$ is scanned towards more negative voltages, the oscillation period changes to a smaller value when entering region 2. In region 3, the period increases. In

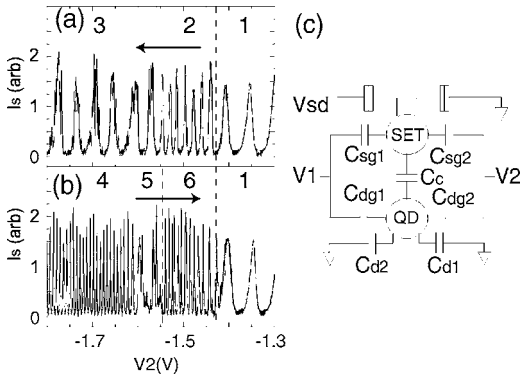

FIG. 3. (a) and (b): The current through Al SET in a scan of $V2$ over 5 min at $V1=-1.4$ V. The arrows indicate the directions of the scan. The bias condition for the other gates ($V_M=-1.267$ V and $Vp=-1.317$ V) is similar to those for Figs. 2. (c) An equivalent circuit representing the device geometry in regions 2–6.

addition, I_s fluctuates causing sharp spikes in each conductance peak [Fig. 3(a)]. Each spike arises from the escape of one electron from the QD. When the scan direction is reversed at $V2=-1.65$ V [Fig. 3(b)], the feature changes in region 4, where I_s is stable without exhibiting any fluctuation and the oscillation period is reduced to a very small value [Fig. 3(b)]. Though not shown here, another remarkable feature of region 4 is that the oscillation pattern of I_s is reproduced when the scan direction is reversed again within this region; viz., it is insensitive to the scan direction as long as the scan range stays within region 4. As $V2$ is scanned towards less negative voltages entering region 5, the oscillation period becomes much larger, and the conductance peak is furnished with sharp spikes. This suggests that electrons flow back to the QD in this region. When entering region 6, the period gets smaller while each conductance peak is accompanied by sharp spikes visible but not clearly seen in the curve of Fig. 3(b). The remarkable feature in region 6, recognized in Fig. 2(b), is that the conductance peak traces are of the opposite slope to those in all the other regions. This is a surprising feature because electrons escape from the Al island of Al SET as gate 2 is less negatively biased.

For modeling the electron system in regions 2 to 6, we apply a simple equivalent circuit shown in Fig. 3(c). The change in the number of electrons, ΔN_{SET}, in the Al island of Al SET with varying V2 is tracked by counting the conductance peaks of Al SET. Figure 4(a) displays the data taken from the curves of I_s vs $V2$ at $V1=-1.18$ V. The numbers mark the different regions. The number of electrons, N_{QD}, in the QD is also derived from the same data by counting the spikes appearing in the conductance resonance peaks of I_s, as displayed in Fig. 4(b). If an electron enters or leaves the QD at each spike it can be identified by the polarity of the spike. The large hysteresis loop in Fig. 4(b) shows that the QD takes two different states with largely different values of N_{QD} in a given bias condition.

We now wish to interpret the experimental findings. Let $U1$ and $U2$ be the electrostatic potential energies at the saddle point of QPC $M1$ and QPC $M2$, and U_{QD} the conduction band bottom of the 2DEG underneath the SET (or QD). In the condition when V_M, V_p, and $V1$ are fixed at constant

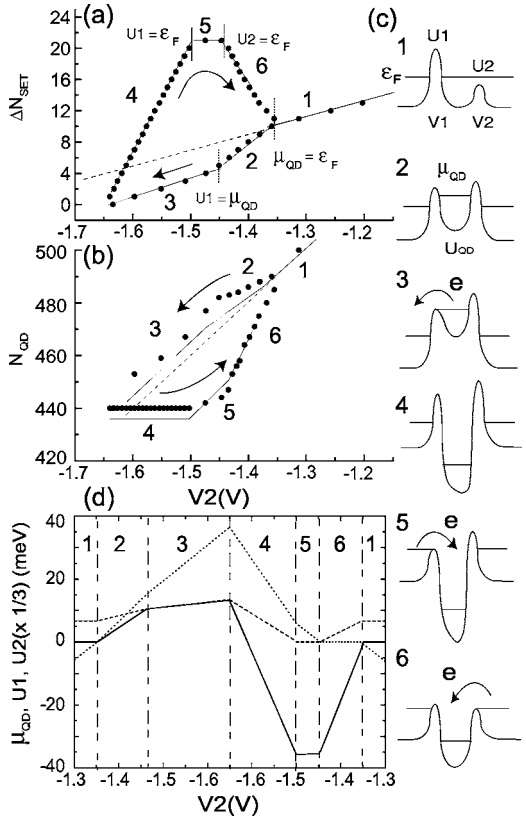

FIG. 4. (a) The change of in number of electrons, ΔN_{SET}, in the Al island of Al SET induced by scanning $V2$. The values are experimentally derived from the data taken at $V1=-1.18$ V, $V_M=-1.304$ V, and $Vp=-1.439$ V. The dashed straight line is extrapolated from the line of region 1 to indicate the equilibrium values of ΔN_{SET}, at which $\mu_{QD}=0$. The solid lines are guides for the eye. (b) The number of electrons in the QD, N_{QD}, derived from the same data as that for (a). The experimental error in counting N_{QD} is ±5. The solid lines show theoretical values derived from the analysis. See the text. (c) Schematic representation of the evolution of important energies relevant to the QD, μ_{QD}, $U1$, $U2$, and U_{QD}. (d) The energies of μ_{QD} (solid line), $U2$ (dotted line), and $U1$ (dashed line) derived from the analysis as a function of $V2$.

values, the quantities, $U2$, $U1$, and U_{QD}, will vary linearly against small changes in $V2$ and N_{QD};[13] hence,

$$\Delta U2 = -e\kappa_{2,2}\Delta V2 + \kappa_{2,QD}\frac{e^2}{C_\Sigma}\Delta N_{QD}, \tag{1}$$

$$\Delta U1 = -e\kappa_{1,2}\Delta V2 + \kappa_{1,QD}\frac{e^2}{C_\Sigma}\Delta N_{QD}, \tag{2}$$

$$\Delta U_{QD} = -e\kappa_{QD,2}\Delta V2 + \frac{e^2}{C_\Sigma}\Delta N_{QD}, \tag{3}$$

where e is the unit charge and $\kappa_{i,j}$ are geometrically determined constants that are kept unchanged in regions 1 through 6. It is important that the inequality relations, $\kappa_{2,2} > \kappa_{QD,2} > \kappa_{1,2}$, hold in the present sample geometry. We begin with a brief sketch of how the energies relevant to the QD evolve as $V2$ is scanned. As illustrated in Fig. 4(c), region 1 is charac-

terized by a finite conductance through QPC $M2$, which imposes $U2 < \varepsilon_F = \mu_{QD}$, where $\varepsilon_F = 0$ is the Fermi level on the leads and μ_{QD} the electrochemical potential of the QD (the highest energy of occupied states). Since one-electron energy-level spacing of the QD is only about 9.6 μeV, we assume $\Delta\mu_{QD} \sim \Delta U_{QD}$ in the following discussion. As gate 2 is more negatively biased, $U2$ increases to eventually reach $U2 = \varepsilon_F$, at which the QD is closed entering region 2. In region 2, ΔN_{QD} is expected to be zero in our model.[14] While $U2$, $U1$, and U_{QD} are all lifted up with more negatively biasing gate 2, the increase of U_{QD} is smaller than that of $U2$ but larger than $U1$ due to $\kappa_{2,2} > \kappa_{QD,2} > \kappa_{1,2}$; hence, both $U1$ and $U2$ are higher than μ_{QD}. As gate 2 is more negatively biased in region 2, μ_{QD} approaches $U1$. When μ_{QD} reaches $U1$, the system moves to region 3, where the rise in U_{QD} forces electrons to tunnel out of the QD ($\Delta N_{QD} < 0$) through QPC $M1$ so that $\mu_{QD} = U1$ is satisfied. Reversing the scan direction of $V2$ immediately stops leaking of electrons out of the QD because $\kappa_{QD,2} > \kappa_{1,2}$: An isolated excited state ($U1, U2 > \mu_{QD}$) of the QD is established in region 4 ($\Delta N_{QD} = 0$). The values of $U2$, $U1$, and U_{QD} at a given value of $V2$ in region 4 are substantially lower than those at the same values of $V2$ in region 2 or 3 because a certain amount of electrons have been lost from the QD. The bottom of the QD, U_{QD}, goes down faster than $U1$ because $\kappa_{QD,2} > \kappa_{1,2}$, and eventually, μ_{QD} drops below ε_F. When $U1$ is pushed down to reach $\varepsilon_F = 0$, the system makes a transition to region 5, where electrons enter the QD through QPC $M1$. The rate at which electrons enter the QD is determined to be $\frac{\Delta N_{QD}}{\Delta V2} = 250/V$ by replacing $\Delta U1 = 0$ in Eq. (2). As $V2$ is scanned towards still less negative values, $U2$ is pulled down to reach ε_F, at which the system is driven to region 6, where electrons tunnel into the QD through QPC $M2$. The rate at which electrons enter the QD is now determined to be $\frac{\Delta N_{QD}}{\Delta V2} = 460/V$ by replacing $\Delta U2 = 0$ in Eq. (1), and the channel through QPC $M1$ is closed. $U1$, U_{QD}, and μ_{QD} rise up because $\Delta N_{QD} > 0$, while $U2 = 0$ is retained. When μ_{QD} reaches $\varepsilon_F = 0$, the system returns to region 1.

The scenario in the above is supported by the following quantitative discussion. First, we derive values of ΔU_{QD} directly from experimental values of ΔN_{SET} [Fig. 4(a)] through[15]

$$\Delta N_{SET} = (C^1_{sg2}/e)\Delta V2 + (C_c/e^2)\Delta U_{QD}. \quad (4)$$

Here, C^1_{sg2} is a coefficient to be derived when $U_{QD} = 0$: It is evaluated to be $C^1_{sg2} = 3.12$ aF from the experimental value $\frac{\Delta N_{SET}}{\Delta V2} = 20/V$ found in region 1. This coefficient, as well as $C_c = 58.8$ aF, is a geometrically determined constant. These coefficients, including those in Eqs. (1)–(3), may vary slightly as $V2$ is scanned. We expect, however, that the possible variation is less than 5%.[13] Assuming constant coefficients, we can derive values of $\Delta U_{QD} = \Delta\mu_{QD}$ without using any adjustable parameters: The solid lines in Fig. 4(d) show the derived values in the respective regions. Second, we rewrite $\Delta U1$ and $\Delta U2$ in Eqs. (1) and (2) as a function of $\Delta V2$ and ΔU_{QD} using Eq. (3). Knowing the values of ΔU_{QD}, and imposing experimentally found values of $V2$ for the transition points between adjacent regions [Fig. 4(a)], we can find that $\kappa_2 = \kappa_{2,2} - \kappa_{2,QD}\kappa_{QD,2} = 0.33$, $\kappa_{2,QD} = 0.885$, $\kappa_1 = \kappa_{1,2} - \kappa_{1,QD}\kappa_{QD,2} = 0.0122$, and $\kappa_{1,QD} = 0.23$. The values in the above are uniquely determined to reproduce the transition points. By summing up $\Delta U1$ and $\Delta U2$ in each region, we derive values of $U1$ and $U2$ as shown by the dashed and the dotted lines, respectively, in Fig. 4(d). Possible variation in the coefficients (5%) make us roughly estimate that the relative accuracy of energy values is 10% in Fig. 4(d). The features of $\Delta U2$, $\Delta\mu_{QD}$, and $\Delta U1$ correctly reproduce the behaviors discussed already. Finally, we check the consistency of our treatment by quantitatively evaluate ΔN_{QD} from Eq. (3), where the coefficient, $\kappa_{QD,2} = 0.33$, is uniquely determined by the value $\frac{\Delta U_{QD}}{\Delta V2} = -0.33\ e$ in region 4. The theoretical values obtained by assuming $C_\Sigma \sim 106$ aF are shown by the solid lines in Fig. 4(b). The excellent agreement between the theoretical and the experimental values strongly supports the validity of our model discussed here. The parameter value, $C_\Sigma = 106$ aF, is substantially smaller than the value, $C_\Sigma = 262$ aF, obtained in region 1. This is reasonable because the capacitance coupling to the source and the drain leads, dominant in region 1, nearly vanishes in regions 2 through 6.

We should mention the small discrepancy in region 2, where $\Delta N_{QD} = 0$ was expected in our model but N_{QD} slowly decreases with decreasing $V2$. Actually, we suppose that the QD is squeezed with decreasing $V2$.[16] Therefore, μ_{QD} is expected to rise up more rapidly than $U2$ does. It follows that electrons escape from QD so as to satisfy $\mu_{QD} = U2$ in region 2. As shown in Fig. 4(d), the present analysis suggests that (i) μ_{QD} is lifted up in region 3 to reach a value as high as 13 meV above ε_F at $V2 = -1.65$ V, and (ii) μ_{QD} falls down rapidly in region 4 until it reaches a value as low as ~ -36 meV below ε_F when region 5 is reached. The large departures of μ_{QD} from ε_F in the above might seem to be surprising at first sight. We stress, however, that these are the consequence readily understandable from the fundamental electrostatics, without invoking detailed analysis. If a QD were tunnel coupled to reservoirs as in standard transport measurements of Coulomb blockade oscillations, or in region 1, μ_{QD} would be tightly bound to ε_F, staying within a narrow energy range a half of the charging energy below or above ε_F. This is because, in a given gate bias condition, the QD takes either one of the two states in which N_{QD} can differ only by one. The situation is totally different in the isolated QD: N_{QD} can differ largely between the two states in the same gate bias condition. For instance, at $V2 = -1.5$ V in Fig. 4(b), N_{QD} differs by as large as 32 between one state in region 3 and the other state in region 4. Note that the gate bias condition is the same between the two states. This immediately implies that μ_{QD} differs by a value approximately 32 times as large as the charging energy. The charging energy is expected to be substantially larger than 0.6 meV, which is experimentally derived in region 1. Thus the values of μ_{QD} shown in Fig. 4(d) are reasonable quantitatively. The rapid fall of μ_{QD} with increasing $V2$ in region 4 is caused by the lack of screening ($\Delta N_{QD} = 0$). The negative-energy state in region 5 ($\mu_{QD} < 0$) occurs because the QD is completely isolated. To our knowledge, this kind of negative-energy state has never been reported in the earlier literatures. In region 6, the rate at which electron enters the QD, $\frac{\Delta N_{QD}}{\Delta V2}$

$=460/V$, is so high that U_{QD} does increase and N_{SET} decreases as gate 2 is less negatively biased. In other words, the QD is more negatively charged up if $V2$ is scanned towards the positive direction.

We have confirmed that the electrons in the excited QD ($\mu_{QD}>0$) are of a very long lifetime (>20 min), by monitoring time traces of I_s in region 4. The excited state of a QD with $\mu_{QD}>0$ has been studied and an analogy to a radioactive nuclei exhibiting sequential α decay processes is suggested.[17,18] The negative-energy state of the QD with $\mu_{QD}<0$ might be viewed as an energy sinker for a surrounding electron system. The current flowing into an isolated QD with $\mu_{QD}<0$ will cool down the electron temperature of the surrounding electron system. By appropriately arranging multiple QD systems, therefore, the QD might find application for implementing nano-scale on-chip cryogenics.[19] In general these long-lived electron states in the QD may also provide a clean system for an information processing unit. For instance, the information can be input into the QD from Al SET when the QD is electrically isolated. For two isolated dots, quantum entanglement between two electronic states could even be realized.

In summary, we have studied electronic properties of an isolated QD by using an Al SET fabricated on top as a probe to the QD. By controlling potential barriers defining the QD, several characteristic regimes of the electronic state have been identified. The data suggest the existence of excited isolated QD states with both positively lifted up and negatively sinking energies.

We thank O. Astafiev, L. Kulik, K. Ikushima, Y. Kawaguchi, C. D. Chen, and C. C. Chi for experimental assistance. This work is supported by the Core Research for Evolutional Science and Technology (SORST) of the Japan Science and Technology Corporation (JST).

[1] J. M. Elzerman, R. Hanson, L. H. Willems van Beveren, B. Witkamp, L. M. K. Vandersypen, and L. P. Kouwenhoven, Nature (London) **430**, 431 (2004).

[2] J. M. Elzerman, R. Hanson, L. H. Willems van Beveren, B. Witkamp, L. M. K. Vandersypen, and L. P. Kouwenhoven, Appl. Phys. Lett. **84**, 4617 (2004).

[3] J. A. Folk, C. M. Marcus, and J. S. Harris, Jr., Phys. Rev. Lett. **87**, 206802 (2001).

[4] Eli Eisenberg, Karsten Held, and Boris L. Altshuler, Phys. Rev. Lett. **88**, 136801 (2002).

[5] P. Kleinschmidt, S. Giblin, A. Tzalenchuk, H. Hashiba, V. Antonov, and S. Komiyama (unpublished).

[6] S. Gardelis, C. G. Smith, J. Cooper, D. A. Ritchie, E. H. Linfield, Y. Jin, and M. Pepper, Phys. Rev. B **67**, 073302 (2003).

[7] Wei Lu, Zhongqing Ji, Loren Pfeiffer, K. W. West, and A. J. Rimberg, Nature (London) **423**, 422 (2003).

[8] W. Lu, A. J. Rimberg, K. D. Maranowski, and A. C. Gossard, Appl. Phys. Lett. **77**, 2746 (2000).

[9] D. Berman, N. B. Zhitenev, R. C. Ashoori, and M. Shayegan, Phys. Rev. Lett. **82**, 161 (1999).

[10] T. A. Fulton and G. J. Dolan, Phys. Rev. Lett. **59**, 109 (1987).

[11] M. T. Tuominen, J. M. Hergenrother, T. S. Tighe, and M. Tinkham, IEEE Trans. Appl. Supercond. **3**, 1972 (1992).

[12] Y. Nakamura, C. D. Chen, and J. S. Tsai, Phys. Rev. B **53**, 8234 (1996).

[13] Two points should be noted. First, in more accurate terms, the quantities, $U2$, $U1$, and U_{QD}, are linear functions of $V2$, N_{QD}, and N_{SET}. In Eqs. (1)–(3), coefficients $\kappa_{i,j}$ are renormalized through Eq. (4), so that the contribution from ΔN_{SET} is included in these equations. Second, the linear approximation here is admissible because the change of the number of electrons in the QD is only 10% in the experiments and hence the geometrical size (electrical diameter) of the QD is expected to change roughly by only 5%. So the geometrical coefficients in the analysis can be assumed to be approximately a constant with a tolerance of 5%.

[14] This is not consistent with the experimental data [Fig. 4(b)]. As discussed later, the discrepancy does not significantly affect the following arguments.

[15] Equation (4) is the manifestation that the electrochemical potential of SET, μ_{SET}, is bounded by the small charging energy of Al SET, and hence, is safely approximated by $\mu_{SET}=0$ in the present analysis. See also Ref. 13.

[16] With decreasing $V2$, the Coulomb potential penetrates into the interior region of the QD. The profile of electrostatic potential, accordingly, changes to squeeze the electrical size of the QD. In the analysis, however, we do not take account of this effect because such a size reduction cannot be much larger than 5% in relative magnitude (Ref. 13), and does not substantially affect the predictions of the present model.

[17] J. Cooper, C. G. Smith, D. A. Ritchie, E. H. Linfield, Y. Jin, and H. Launois, Physica E (Amsterdam) **6**, 457 (2000).

[18] J. Martorell, D. W. L. Sprung, P. Machado, and C. G. Smith, Phys. Rev. B **63**, 45325 (2001).

[19] J. P. Pekola, R. J. Schoelkopf, and J. N. Ullom, Phys. Today **57**, 41 (2004).